Direct calculations of the CH4+CO2 far infrared collision-induced absorption

Wissam Fakhardji, Christian Boulet, Ha Tran, Jean-Michel Hartmann

Version of Record: https://www.sciencedirect.com/science/article/pii/S0022407322000851
Manuscript_86075af2105d6e62af8a489e0ace0f7e

Direct calculations of the CH_4+CO_2 far infrared collision-induced absorption

Wissam Fakhardji[1], Christian Boulet[2], Ha Tran[1], Jean-Michel Hartmann[1,#]

[1]Laboratoire de Météorologie Dynamique/IPSL, CNRS, École polytechnique, Institut polytechnique de Paris, Sorbonne Université, École normale supérieure, PSL Research University, F-91120 Palaiseau, France.
[2]Institut des Sciences Moléculaires d'Orsay, CNRS, Université Paris-Saclay, Orsay F-91405, France.
[#]Corresponding author: jean-michel.hartmann@lmd.ipsl.fr, orcid.org/0000-0003-3687-989X

ABSTRACT

We present computations, solely using input data from the literature and thus free of any adjusted parameter, of the far infrared collision-induced absorption (CIA) by interacting CH_4 and CO_2 molecules. They are based on classical molecular dynamics simulations (CMDS) of the rotational and translational motions of the molecules made using an accurate ab initio CH_4-CO_2 anisotropic intermolecular potential, and on a long-range expansion of the interaction-induced dipole. Various desymmetrization procedures, which all ensure detailed balance of the spectral density function are a posteriori applied to the CMDS results. The comparison with the available measurements, which have been collected at room temperature, show that a good agreement can be obtained without introducing any ad hoc short-range dipole components, and it enables to point out the limits of some of the desymmetrization procedures. Tests are also made of the so-called "isotropic approximation", which point out its strong limits, since it leads to large underestimations of the CIA, and question previous computations made using an isotropic potential and long-range expansion of the induced dipole complemented by ad hoc contributions at short distances. Finally, the temperature dependence of the CIA is predicted for applications to planetary atmospheres.

1. Introduction

It has been recently suggested [1] that the presence of methane (and hydrogen) in the atmosphere of early Mars could, through the contribution of the CH_4+CO_2 (and H_2+CO_2) collision-induced absorption (CIA) in the far infrared, sufficiently enhance the greenhouse effect to enable water in the liquid phase on the planet surface. This has stimulated the first laboratory measurements [2], quickly followed by a second experimental investigation with reduced uncertainties [3]. Since the measurement were limited to room temperature and because applications to planetary atmospheres require temperature-dependent data, calculations of the collision-induced absorption were also made in [3] using the so-called "isotropic approximation" [4,5], thus neglecting the anisotropy of the CH_4+CO_2 (and H_2+CO_2) intermolecular potential. This approximation, with which the molecular rotation remains unchanged regardless of collisions, is known [5] to underestimate the CIA, particularly for

molecular pairs involving strongly anisotropic forces. In order to obtain agreement with measurements, ad-hoc (but generally wrong) isotropic intermolecular potentials are often used, and empirically short-range contributions to the induced dipole are introduced in order to obtain agreement with measurements (see e.g. [3, 6]). This procedure is thus highly dependent on the availability of precise experimental CIA data and, if only room temperature measurements can be used for the tuning of the computations, extrapolations to other temperatures are hazardous. This being the situation of the theoretical study of [3], there is a strong need for direct computations of the CH_4+CO_2 CIA using an accurate anisotropic intermolecular potential and, if possible, a precise induced-dipole moment surface.

This is precisely what the present paper attempts to do. For this, classical molecular dynamics simulations have been carried in order to predict the time-dependent rotational and translational dynamics of mixtures of CO_2 and CH_4 molecules, based on an accurate ab initio potential [7]. For the dipole induced in interacting (CH_4-CO_2) pairs, and in the absence of any usable (i.e. parameterized as a function of the intermolecular distance and molecules orientations) ab initio results, the long-range expansion given in [8] was used, which likely includes most of the dominant contributions. The theoretical model and data used are presented in Sec. 2. We then compare our predictions with the measurements and with the results of calculations made using the isotropic approximated presented in [3] (Sec. 3.1), discuss the effects of this approximation on the calculated CIA spectra (Sec. 3.2), and investigate the influence of temperature (Sec. 3.3). Concluding remarks and suggestions for future investigations are finally given in Sec. 4

2. Calculations

2.1 Classical molecular dynamics simulations

Classical molecular dynamics simulations (CMDS) were performed for CH_4+CO_2 mixtures at a total density of d and different temperatures T. After choosing the number N of molecules to be treated, the initial positions of their centers of mass, defined by $\vec{P}_{\mathrm{m}}(t=0)$ for molecule m, are randomly chosen in a cubic box of side length $(N/d)^{1/3}$ with the constraint that they should be at least 6 Å away from each other (in order to avoid un-physical situations involving very close pairs). The associated translational velocity $\dot{\vec{P}}_{\mathrm{m}}(t=0)$ is set with a random orientation and a modulus such that the associated energies $M_{\mathrm{m}} \| \dot{\vec{P}}_{\mathrm{m}}(t=0) \|^2 / 2$ (M_{m} being the molecular mass) satisfy the Boltzmann distribution for the considered temperature. Simultaneously, for each CO_2 molecule, its axis orientation is set randomly, defined by a unit vector $\vec{u}_{\mathrm{m}}(t=0)$ along the C-O bond while its angular momentum is set by defining a vector $\dot{\vec{u}}_{\mathrm{m}}(t=0)$ perpendicular to $\vec{u}_{\mathrm{m}}(t=0)$ and of magnitude

such that the associated rotational energies $I(CO_2)\|\dot{\vec{u}}_m(t=0)\|^2/2$, with $I(CO_2)$ the moment of inertia, satisfy the Boltzmann distribution. For each CH_4 molecule, its orientation is set randomly through the choice of three Euler angles $\theta_m(t=0)$, $\phi_m(t=0)$ and $\psi_m(t=0)$ from which the four quaternions $q_{m,i=0,3}(t=0)$ and the rotation matrix $A_m(t=0)$ from the space-fixed (laboratory) to the body-fixed (molecular) frame and are computed according to Eqs. (3.35) and (3.36) of [9]. At the same time, the components of the angular speed vector $\vec{\omega}_m(t=0)$ in the $(\vec{x},\vec{y},\vec{z})$ molecular frame of principal axes are defined such that the associated rotational energies $I_{\alpha\alpha}(CH_4)[\vec{\omega}_m(t=0).\vec{\alpha}]^2/2$, with $\vec{\alpha}=\vec{x}$, $\vec{y}$, or $\vec{z}$ and $I_{\alpha\alpha}(CH_4)$ the components of the moment of inertia tensor, satisfy the associated Boltzmann distributions. Once this initialization step is completed, the propagation in time of the parameters defining the rotational and translational states of all molecules is carried as follows. At each time *t*, we first compute the force $\vec{F}_m(t)$ and torque $\vec{\tau}_m(t)$ in the laboratory frame exerted on each molecule m by its neighbors (within a conservative cut-off distance of 10 Å) by using an input (see below) site-site intermolecular potential. The positions of the sites in the laboratory frame needed for this are directly obtained, for CO_2, from knowledge of the above defined vectors $\vec{P}_m(t)$ and $\vec{u}_m(t)$. For CH_4, the site positions relative to the center of mass in the laboratory frame are obtained from those in the molecular frame by applying the rotation matrix $A_m(t)^{-1} = {}^tA_m(t)$ [see Eq. (3.25) of [9]] computed from the quaternions $q_{m,i}(t)$, and the absolute positions are then deduced by simply adding $\vec{P}_m(t)$ to the result. Once $\vec{F}_m(t)$ is known, the center of mass velocity $\dot{\vec{P}}_m(t+dt)$ is directly obtained from $\dot{\vec{P}}_m(t)$ and the acceleration $\ddot{\vec{P}}_m(t+dt)=\vec{F}_m(t)/M_m$, while $P_m(t+dt)$ is computed from $\vec{P}_m(t)$ and $\dot{\vec{P}}_m(t)$. In order to determine the rotational parameters at *t*+*dt*, different procedures are used for CO_2 and CH_4. For the linear molecule, $\dot{\vec{u}}_m(t+dt)$ and $\vec{u}_m(t+dt)$ are obtained from knowledge of $\vec{\tau}_m(t)$ in the laboratory frame by using Eq. (3.41)-(3.46) of [9]. In the case of the non-linear methane, the torque in the molecular frame is first computed from $\vec{\tau}_m(t)$ by applying the rotation matrix $A_m(t)$ (Eq. (3.30) of [9]). Equations (3.29a)-(3.29c) of [9] are then used to compute the derivatives $\dot{\vec{\omega}}_{m,\alpha=x,y,z}(t)$ of the angular speed component in the molecular frame which, together with $\vec{\omega}_{m,\alpha=x,y,z}(t)$, enable to deduced $\vec{\omega}_{m,\alpha=x,y,z}(t+dt)$. At the same time, the derivative $\dot{q}_{m,i=0,3}(t)$ of the quaternions, computed from knowledge of the $\vec{\omega}_{m,\alpha=x,y,z}(t)$ using Eq. (3.37) of [9], enable to obtain $q_{m,i=0,3}(t+dt)$ from $q_{m,i=0,3}(t)$.

2.2 Collision-induced dipole

The components $\mu_{X,Y,Z}(t)$ in the laboratory frame of the interaction-induced dipole $\vec{\mu}(t)$ in colliding (CH_4,CO_2) pairs was computed following [8], i.e.:

$$\mu_X(t)=[\mu_{-1}(t)-\mu_{+1}(t)]/\sqrt{2}\ ;\ \mu_Y(t)=i[\mu_{-1}(t)+\mu_{+1}(t)]/\sqrt{2}\ ;\ \mu_Z(t)=\mu_0(t)\ , \qquad (1)$$

with:

$$\mu_{n=-1,0,+1}(t)=\frac{4\pi}{\sqrt{3}}\sum_{\substack{a,b,\lambda,L,\\ m,m',m'',q}}(2a+1)D_{a,b,\lambda,L;m'}[R_{CH4\text{-}CO2}(t)]D^{a}_{m,m'}[\theta_{CH4}(t),\phi_{CH4}(t),\psi_{CH4}(t)]^{*} \qquad (2)$$
$$\times Y^{b}_{m''}[\theta_{CO2}(t),\phi_{CO2}(t)]Y^{L}_{M-q}[\theta_{CH4\text{-}CO2}(t),\phi_{CH4\text{-}CO2}(t)]<abmm''|\lambda q><\lambda LqM\text{-}q|lM>\ .$$

In this equation, $D^{a}_{m,m'}[\theta_{CH4}(t),\phi_{CH4}(t),\psi_{CH4}(t)]^{*}$ denotes the conjugate of the complex Wigner rotation for the Euler angles defining the orientation of the CH_4 molecule, while $Y^{b}_{m''}[\theta_{CO2}(t),\phi_{CO2}(t)]$ and $Y^{L}_{M-q}[\theta_{CH4\text{-}CO2}(t),\phi_{CH4\text{-}CO2}(t)]$ are spherical harmonic dependent on the angles defining the orientations of the CO_2 molecule and of the axis between the centers of mass of the pair, respectively, and <….|..> are Clebsch-Gordan coefficients. The $D_{a,b,\lambda,L;m'}[R_{CH4\text{-}CO2}(t)]$ depend on the intermolecular distance $R_{CH4\text{-}CO2}(t)$ and type of dipole-induction process. Their expressions in terms of intrinsic parameters (e.g. electric multipoles, polarizabilities, ..) of the CH_4 and CO_2 molecules are provided in [8] where their numerical values are also given, computed from a set of molecular parameters listed in the same article. The sum in Eq. (2) thus runs over the 39 $(a,b,\lambda,L;m')$ sets given in Table IV of [8], complemented by the associated values of m, m" and q allowed by the Clebsch-Gordan selection rules.

2.3 Absorption spectrum

The above described CMDS and induced-dipole expressions provide the dipole $\vec{\mu}(t)$ at all times, whose autocorrelation function in the low density limit:

$$ACF(t-t_0)=\sum_{i=CH_4}\sum_{j=CO_2}\vec{\mu}_{i,j}(t_0).\vec{\mu}_{i,j}(t)\ \text{ for } t\geq t_0 \qquad (3)$$

can be obtained after an initial time t_0 has been chosen [note that equation (3), which disregards cross terms associated with different CH_4 (or CO_2) molecules, is here valid because, at the considered low density, intermolecular collisions are (practically) purely binary and uncorrelated]. From the latter, the absorption coefficient at angular frequency ω (ω=2πcσ where σ is the wavenumber in cm^{-1}), for the temperature *T* and molecules density *d*, is given, in units of length^{-1}, by [4,5]:

$$\alpha(\omega)=A\frac{4\pi^2}{3\hbar c}f_D(\omega)\omega[1-e^{-\hbar\omega/k_bT}]\frac{1}{V}C(\omega) \quad (4)$$

where *V*= *N/d* is the volume associated with the number of molecules (*N*) and density (*d*) chosen for the calculations. *A* is a conversion factor [$A=(e.a_0)^2/(4\pi\varepsilon_0)$], e being the electron charge ($\approx 1.6\ 10^{-19}$ C),

a_0 the Bohr radius (≈5.3 10^{-11} m) and ε_0 (≈8.85 10^{-12} $C^2/(Jm)$) the vacuum permittivity] to switch from atomic units used for the induced dipole to SI units, and C(ω) is given by:

$$C(\omega) = \mathrm{Re}\left\{\frac{1}{\pi}\int_0^{t_{Max}-t_0} ACF(t)e^{-i\omega t}dt\right\} = \frac{1}{\pi}\int_0^{t_{Max}-t_0}\cos(\omega t)ACF(t)dt \quad (5)$$

where t_{Max} is the ending time of the CMDS. In Eq. (4), $f_D(\omega)$ is the desymmetrization function needed to insure the respect of the detailed balance relation or the fluctuation-dissipation theorem, i.e. the fact that one should have $C(+\omega)/C(-\omega) = \exp(\hbar\omega/k_B T)$ [5]. This is required since the CMDS only provide the dipole ACF for positive times and thus cannot satisfy the relation $ACF(-t) = ACF(+t - i\hbar/k_B T)$ which leads to the above given detailed balance relation. The different procedures that we used are:

P-1: $f_D^{(1)}(\omega) = \dfrac{2}{1+e^{-\hbar\omega/k_B T}}$, (6)

P-2: $f_D^{(2)}(\omega) = \dfrac{\hbar\omega}{k_b T}\dfrac{1}{1-e^{-\hbar\omega/k_B T}}$, (7)

P-3: $f_D^{(3)}(\omega) = e^{\hbar\omega/2k_B T}$, (8)

and

P-4: $f_D^{(4)}(\omega) = \dfrac{e^{\hbar\omega/2k_B T}ACF(0)}{C(\omega)ACF\left[\hbar/(\sqrt{2}k_B T)\right]}\int_0^{t_{\max}-t_0} ACF\left[\sqrt{t^2+(\hbar/2k_B T)^2}\right]\cos(\omega t)dt$. (9)

The first two are reported in [4] without information of who originally proposed them and they seem to have been rarely (if not never) used. The third, known as the Schofield's procedure [10], has been widely used and was applied in classical calculations of the CIA of pure CO_2 [11] and N_2 [12, 13] and, recently of (CH_4,N_2) pairs [14], for instance. Finally, the P-4 procedure, which corresponds to that initially proposed by Egelstaff [15] as modified by Frommhold [4] who added the scaling factor $ACF(0)/ACF\left[\hbar/(\sqrt{2}k_B T)\right]$, was used in [14, 16], for instance. Recall that [17] showed that Egelstaff's correction well describes the quantum mechanical rotational spectrum of freely rotating linear molecules. It is important to note that all procedures being a posteriori corrections they are approximate, and that choosing the best one is not straightforward since it may depend on the temperature and/or the spectral domain of interest.

2.4 Implementation and data used

CMDS were carried at various temperatures for a 50%CO_2+50%CH_4 mixture at a total density of *d*=2 amagat (1 amagat corresponding to 2.687 10^{25} molec/m^3). Numerous simulation boxes, each containing 20,000 molecules, were treated sequentially, using periodic boundary conditions and closest neighbor spheres [9], leading to a total number of at least 20 million particles. In order to save

CPU time, only CO_2-CH_4 interactions were taken into account using the accurate site-site ab initio anisotropic potential of [7]. This approximation is valid, since at the moderate density retained, collisions involving three molecules are extremely rare and can be disregarded. After initializations, computations were carried up to t_{Max}=105 ps with a temperature-dependent time step small enough to accurately describe the rotational and translational motions, and time origin t_0=100 ps was retained for the computation of the dipole ACF. This value of the thermalization delay was chosen from analysis of the convergence of the radial distribution function. The dipole ACF was thus computed over a time interval of $t_{\mathrm{Max}} - t_0$=5 ps, which implies that the Fourier Laplace transform in Eq. (5) is truncated in time. The computed spectrum is thus the convolution of the true one by a $\mathrm{sinc}[2\pi c\sigma(t_{\mathrm{Max}} - t_0)]$ function, which has negligible consequences since the latter (which has a full width at half maximum of about 4 cm^{-1}) is much narrower than the spectrum. In the calculations, a cut-off distance of 10 Å was retained for interacting pairs with the same criterion applied for the computation of the induced dipole through the sums in Eq. (3). The equilibrium geometries were used for the CO_2 and CH_4 molecules which were treated as rigid rotors. For the induced dipole, the 39 $D_{a,b,\lambda,L;m'}[R_{\mathrm{CH4\text{-}CO2}}(t)]$ parameters given in Table IV of [8], which depend on the intermolecular distance $R_{\mathrm{CH4\text{-}CO2}}(t)$ and type of dipole-induction process, were used without modification.

3. Results and discussion

3.1 Comparison with experimental data and previous computations at T=300K

We performed simulations at *T*=300 K to compute the absorption coefficient and compare it with available experimental and computed results [3]. For this, we tested the four desymmetrization procedures presented in section 2.3 [Eqs. (6)-(9)] in order to evaluate them. The corresponding results, displayed in Fig. 1, call for several remarks. (i) The first is that the various desymmetrization procedures lead to roughly equivalent spectra up to ~100 cm^{-1} with differences that increase at high frequencies, as could be expected from their dependences on $\hbar\omega/2k_{\mathrm{B}}T$. This result is similar to the one found for CH_4-N_2 in [14] where the authors noticed the same behavior. (ii) The second is that P-2 and P-3 are those which lead to the best consistency with experimental data (within the associated error bars, except at low frequencies). It is worth noting that no ad hoc short-range dipole contributions are here needed to obtain agreement with measurements. (iii) Thirdly, significant differences are obtained between our results and those calculated in [3]. However, note that the latter have been obtained using the isotropic approximation and empirical short-range dipole contributions. As further discussed in the next section, by their isotropic nature, such computations strongly underestimate the absorption, which requires the use of both an ad hoc (and wrong) isotropic potential and the adding, as previously done for CH_4-N_2 [6] for instance, of some short-range dipole components in order to obtain agreement with the experimental data. (iv) Finally, the remarks above

raise the question of the "trueness" of the bump in the measured spectra around 300 cm^{-1} since it is not predicted by our computations and is neither observed [18] nor calculated [6, 14] in the case of CH_4-N_2. This demonstrates the need for new measurements of the far infrared absorption by CH_4+CO_2 mixtures.

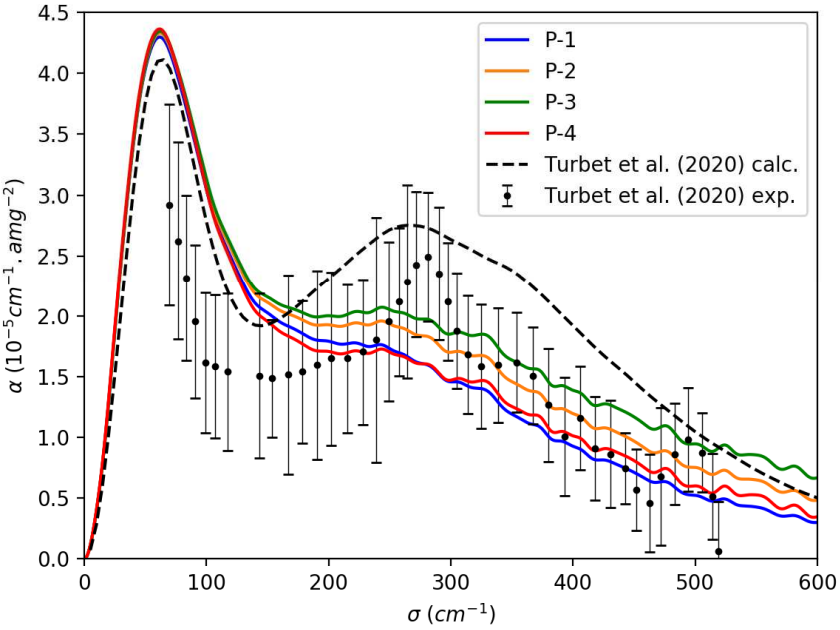

Figure 1: Density normalized CH_4-CO_2 binary absorption coefficients at T=300 K. The blue, orange, green and red lines are the values obtained in the present study using the desymmetrization procedures P-1, P-2, P-3, and P-4, respectively. The experimental data from [3] are shown with black dots and error bars. The dashed black line represents the values calculated in [3] using empirical estimated short-range components of the dipole.

3.2 Effect of the potential anisotropy

In theoretical approaches of the CIA, the use of an isotopic potential greatly simplifies the formalism, but it is known that, when the intermolecular potential anisotropy is large, this approximation may lead to largely underestimated computed spectra [4,5]. As demonstrated below, it is the case for the CH_4-CO_2 system considered in this study. A first indication of this is given by Fig. 2 which displays the interaction energy for various intermolecular distances R and a dense and uniform sampling of the orientations (in order to provide a good sampling of the phase space) computed using the potential of [7] [Note that results for specific configurations can be found in Fig. 2 of [7] which demonstrates that the orientation of CO_2 has a bigger influence on the potential than that of the spherical top CH_4]. Indeed, as already noted in [7] and shown by Fig. 2, the position of the repulsive front (and of the minimum) significantly varies from one angular configuration to another, with distances for which the potential is zero ranging from about 3.0 to 4.5 Å. Now recall that dominant contributions to the induced dipole moment come [8] from the matrix elements D(0223;0) and D(3034; +/-2) in Eq. (2) which vary as R^{-4} and R^{-5}, respectively. This implies that the dipole ACF for a pair of colliding molecules is a highly nonlinear and quickly decreasing function of the distance and

thus that its value computed using the mean (isotropic) potential will be significantly smaller than the true average ACF obtained taking the potential anisotropy into account. Another way to say this is that interactions at short distances make a much larger contribution than those at larger separation to the dipole, while the two essentially contribute with the same weight in the isotropization of the potential. From this one can expect (as confirmed below), that disregarding the potential anisotropy will strongly underestimate the absorption and that agreement with measurements can only be obtained, within the isotropic approximation, by using a potential wrongly and significantly shifted toward close distances (see Fig. 2).

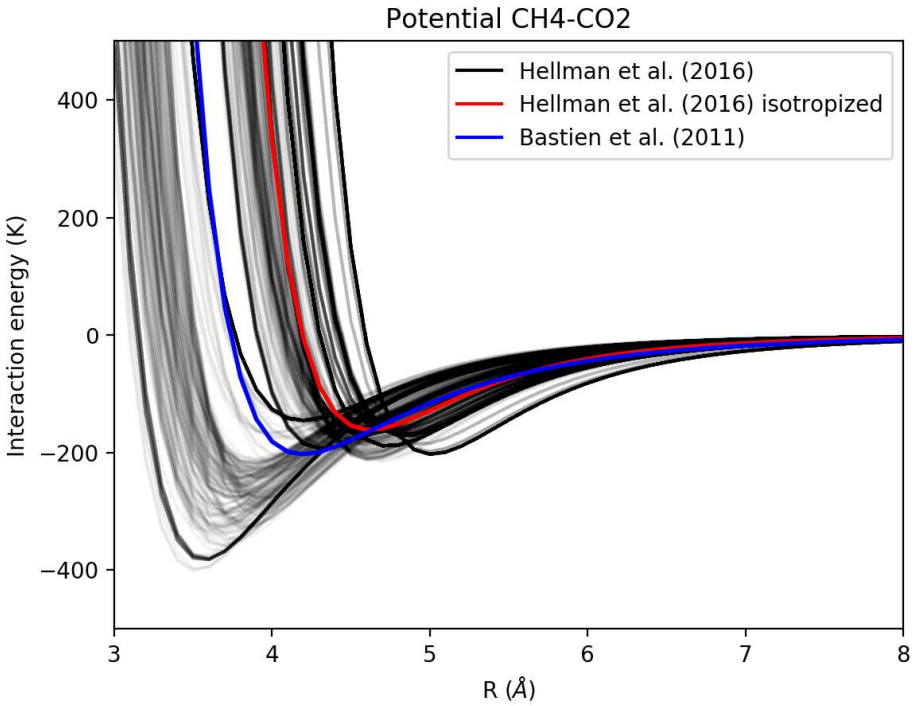

Figure 2: CH_4-CO_4 interaction energies as a function of the distance R between the centers of mass of the two molecules. The values for various molecular orientations, computed using the anisotropic potential of [7], are shown by the grey lines, while the isotropic component, obtained by averaging, is represented by the red line. The isotropic potential used in [3] is represented by the blue curve.

In order to confirm these statements, we have "isotropized" the anisotropic potential of [7] by averaging it over all possible angular configurations of both CH_4 and CO_2 for fixed distances between the centers of mass of the two molecules. The result was then fitted with a modified version of a Hartree-Fock dispersion (HFD) potential, developed by [19] and used previously for the molecular dynamics computation of CIA spectra for rare gases in the liquid phase [20]. The expression of this pair potential is:

$$V(R) = \varepsilon\left\{Ae^{-\alpha x} - \left(C_6/x^6 + C_8/x^8 + C_{10}/x^{10}\right)F(x)\right\}\ , \tag{10}$$

where $x \equiv R/r_m$ and:

$$F(x) = \exp[-(D/x-1)^2] \text{ for } x < D, \text{ while } F(x) = 1 \text{ for } x \geq D\ . \tag{11}$$

The parameters obtained thanks to a Levenberg-Marquardt least square minimization procedure are: r_m=4.6 Å, ε=162 K, A=1066968., α=13.2273, C_6=3.238, C_8=-9.596, C_{10}=11.549, and D=1.758. Note that -ε and r_m are respectively the value of the potential minimum and the distance for which it is obtained. In Fig. 2, we show a comparison between this isotropized potential and the 12-6 Lennard-Jones isotropic potential, originally developed in [21], used in [3]. As can be seen, while their respective depths are quite consistent (203 K and 162 K, respectively), the repulsive front of the isotropic potential used in [3] is significantly shifted to the left, the distance for which it is zero being about 3.7 Å against 4.2 Å for the isotropic component of Hellman's potential [7]. This implies that the former will allow colliding CH_4 and CO_2 molecules to get (unrealistically) closer, thus resulting in a stronger dipole moment and absorption, (artificially) compensating for the errors associated with the use of the isotropic approximation in the computed CIA spectrum.

This statement is confirmed by the results in Fig. 3, where the results obtained using the anisotropic potential of [7] and the associated isotropized one show that the isotropic calculation largely underestimates the magnitude of the absorption coefficient. It is interesting to note that the relative effect of the potential anisotropy significantly varies with the wavenumber, as it is less pronounced for the first peak around 60 cm^{-1} than for the barely discernable second one around 250 cm^{-1}. In order to explain this observation, recall that the first peak is mainly due to the polarization of CH_4 by the electric field of the CO_2 quadrupole, which corresponds to the D(0223;0) term and leads to an induced dipole varying as R^{-4}. The second peak results from the polarization of CO_2 by the electric field of the CH_4 octopole, which corresponds to the D(3034; +/-2) terms and leads to an induced dipole varying as R^{-5}. It is thus clear that allowing molecules to get closer will lead to a relative increase of the second peak greater than for the first peak. In order to be a little more quantitative, consider the two isotropic potentials plotted in Fig. 2 and recall that they become positive (i.e. the beginning of the repulsive fronts) around 3.7 and 4.2 A, respectively. For such distances, the squared dipoles due to the two mechanisms discussed above thus change by the ratios $(4.2/3.7)^8$ and $(4.2/3.7)^{10}$, respectively, leading to a change of the absorption at the first peak by a factor of about 2.7 while the change for the second peak is a factor 3.6. These numbers, which are consistent with the differences between the two isotropic results in Fig. 3 (which use the same molecular parameters and interaction-induced dipole contributions, confirm the large role of the potential anisotropy and the fact that, in [3], the errors resulting from the isotropic approximation are partly compensated by the use of a somehow ad hoc intermolecular potential. Note that this statement also applies to the calculations for CH_4-N_2 presented in [6]. Indeed, in this case also, the isotropic Lennard Jones potential used (σ=3.65 Å, ε=90 K) is significantly and wrongly shifted toward closer distances when compared with the isotropic component of the accurate CH_4-N_2 potential of [22] (which intercepts zero at 3.9 A). Note that the CMDS spectra presented in Fig. 3 have been obtained using the Schofield's procedure (P-3, see section 2.3), but similar conclusions would be obtained with the other desymmetrization procedures.

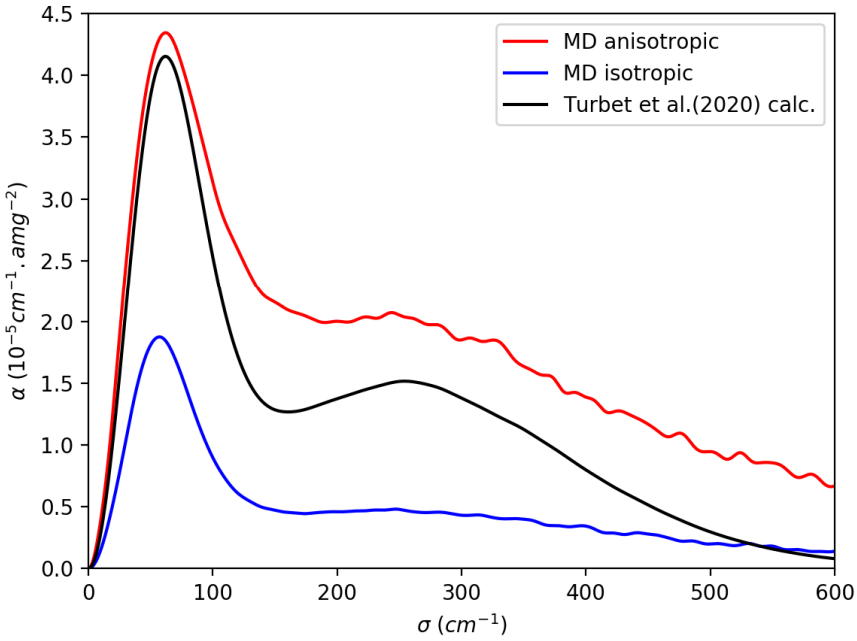

Figure 3: Computed density-normalized CH_4-CO_2 binary absorption coefficients at T=300 K. The red and blue lines are results obtained using the anisotropic potential of [7] and its isotropized version. The black corresponds to the values calculated in [3] without the introduction of the short-range dipole components

It is worth noting that the influence of the anisotropy of the intermolecular potential on the CH_4-CO_2 CIA pointed out by the results in Fig. 3 is much larger than what was found for the few other molecular pairs for which this issue has been investigated. Indeed, the classical [12] and quantum [23] computations of the far infrared CIA spectrum for pure N_2 have demonstrated small anisotropy effects, with a similar conclusion drawn for H_2-He [24] for instance. This can likely be attributed to the fact that N_2 and H_2 are much smaller molecules than CO_2 (and CH_4), which leads to significantly lower influences of the molecules orientations on intermolecular forces at the relatively short distances in the attractive well and repulsive front. This explanation (and influence of CO_2) is supported by the fact that, for H_2-CO_2, the integrated intensity of the roto-translational CIA band computed using an anisotropic potential is significant larger, by a factor of 1.85 at 300 K, than that obtained within the isotropic approximation [3].

3.3 Absorption coefficients for various temperatures

In [3], predictions of the temperature dependence (namely at T=100, 200, 300, 400 and 500 K) of the far infrared CIA by CH_4-CO_2 mixtures were made. They have the merit, at a time when only measurements at room temperature were available, of providing data for planetary studies but, as discussed above, they have the disadvantage of using the isotropic approximation and a wrong potential and were complemented by ad hoc short range induced dipole contributions. Indeed, since using an isotropic intermolecular potential leads to wrong predictions of the collisional dynamics, the

errors in the computed CIA of [3] resulting from this approximations vary with *T*. It is thus likely that these predictions do not well represent the evolution with temperature of the CIA. In order to check this, we carried CMDS computations, still using the anisotropic potential of [7] and the induced-dipole development of [8], for the same temperatures as in [3]. The results obtained are displayed in Figs. 4a-d, calling for the following remarks. (i) The first is that the results for 100 K (Fig. 4a), rule out the use of the desymmetrization procedure P-3 which leads to an unrealistic increase of the CIA in the high frequency tail of the band. This results in this spectral region from the very quick increase of the $f_{\mathrm{D}}^{(3)}(\omega) = \exp(\hbar\omega / 2k_{\mathrm{B}}T)$ factor with decreasing temperature (at 400 cm^{-1}, it varies from 2.6 at *T*=300 K to 18 for T=100 K, with corresponding numbers of 4 and 75 for 600 cm^{-1} !). (ii) The second remark is that, as could be expected, the relative evolution of the absorption with temperature depends on the desymmetrization procedure. (iii) The comparisons between our calculations, for instance obtained with the P-2 correction which leads to satisfactory results at room temperature (Fig. 1), and the predictions in [3] show that the latter predict significantly different temperature effects: a much quicker increase, with increasing *T*, of the absorption around 300 cm^{-1} while the effect on the first peak (near 60 cm^{-1}) is reversed and reduced. Considering the approximate nature of the isotropic calculations and ad hoc short-range dipole component used in [3], we believe that the temperature dependences obtained with this model are questionable and less accurate than our calculations. (iv) Finally, these results stress the crucial need for new experiments investigating the influence of temperature. These would enable to further test our model and help in choosing the "best" desymmetrization procedure as well as to confirm the limits of the isotropic approximation pointed out in the present study. This is relevant since the recent experimental results at 200 and 250 K of [25] have too large uncertainties for any definitive conclusion on these issues. Our computations at 200 K fall within their error bars but the latter are far too large to enable a sufficiently stringent test of our predictions.

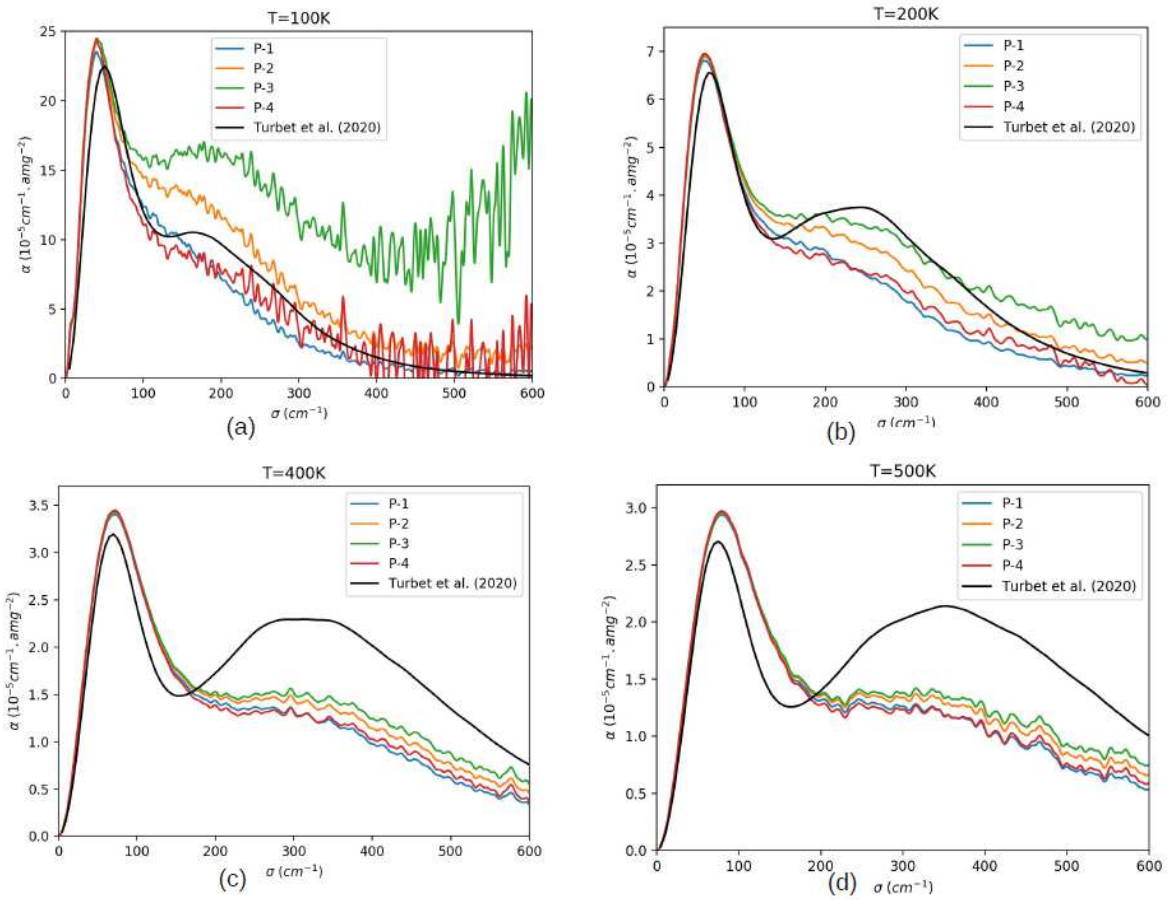

Figure 4: Computed density normalized CH_4-CO_2 binary absorption coefficients at various temperatures. The blue, orange, green and red lines are the values obtained in the present study using the desymmetrization procedures P-1, P-2, P-3, and P-4, respectively. The black line represents the values calculated in [3] using empirical estimated short-range components of the dipole.

4. Conclusion

Classical molecular dynamics simulations of the translational and rotational dynamics in CH_4-CO_2 collisions have been carried using an accurate anisotropic CH_4-CO_2 intermolecular potential. Together with a long-range expansion of the associated interaction-induced dipole, they have enabled calculation of the CH_4-CO_2 binary collision-induced absorption in the far infrared. A good agreement with the available measured values (at room temperature) is obtained without adjusting any parameter (and, in particular without introducing empirical short-range dipole components). This gave confidence in the model, which was thus used to predict CIA values in the 100-600 K temperature range for studies of planetary atmospheres. In addition, various desymmetrization procedures, which all ensure detailed balance of the spectral density function, a posteriori applied to the CMDS results, are tested. This enables to rule out some of them, particularly because they lead to unphysical behaviors at low temperature. Finally, a detailed analysis of the limits of the isotropic approximation, which was used in previous predictions of the CH_4-CO_2 CIA, has been made. It points out and quantifies the large breakdown of calculations made using and isotropic intermolecular potential, and demonstrates that agreement with experimental values can then only be obtained by using an ad hoc and wrong (significantly shifted toward close distances) isotropic potential. Although the long range

expansion of the induced dipole used in the present study likely makes the dominant contribution the CIA, the fact that short range components may also play a role cannot be excluded, particularly at elevated temperature and/or high frequency. Unfortunately, the significant uncertainties on the available measured values do not enable to conclude on this issue, which stresses the crucial need for further experimental studies, if possible more accurate and investigating a broad range of temperatures. In addition, computations of an accurate CH_4-CO_2 interaction-induced dipole would be of great interest, which would enable calculations based on precise dipole and interaction energy surfaces, as recently done with success for the CH_4-N_2 CIA [14, 26].

Acknowledgements
This work was performed in the frame of the *Agence Nationale de la Recherche* (ANR) project COMPLEAT (ANR-19-CE31-0010-01).

Data availability
A table of CIAs at various temperatures, computed as explained in the paper using the P-2 desymmetarization procedure, is available on request to the corresponding author.

Declaration of Competing Interest
The authors declare no conflicts of interest.

CRediT authorship contribution statement
Wissam Fakhardji: Investigation, Formal analysis, Validation, review & editing. **Christian Boulet**: Formal analysis, review & editing. **Ha Tran**: Conceptualization, review & editing. **Jean-Michel Hartmann**: Conceptualization, Writing

References

[1] Wordsworth R, Kalugina Y, Lokshtanov S, Vigasin A, Ehlmann B, Head J, Sanders C, Wang H. Transient reducing greenhouse warming on early Mars. Geophys Res Lett 2017;44:665-71. doi:10.1002/2016GL071766

[2] Turbet M, Tran H, Pirali O, Forget F, Boulet C, Hartmann J-M. Far infrared measurements of absorptions by CH_4+CO_2 and H_2+CO_2 mixtures and implications for greenhouse warming on early Mars. Icarus 2019 ; 321 :189-99. https://doi.org/10.1016/j.icarus.2018.11.021.

[3] Turbet M, Boulet C, Karman T. Measurements and semi-empirical calculations of CO_2+CH_4 and CO_2+H_2 collision-induced absorption across a wide range of wavelengths and temperatures. Application for the prediction of early Mars surface temperature. Icarus 2020;346:113762. https://doi.org/10.1016/j.icarus.2020.113762

[4] L. Frommhold. *Collision Induced Absorption in Gases.* Cambridge Monographs on Atomic, Molecular, and Chemical Physics. Cambridge University Press, Cambridge, (2006).

[5] Hartmann J-M, Boulet C, Robert D. *Collisional effects on molecular spectra: laboratory experiments and models, consequences for applications*. Second Edition, Elsevier, Amsterdam (2021).

[6] Borysow A, Tang C. Far Infrared CIA Spectra of N_2-CH_4 Pairs for Modeling of Titan's Atmosphere. Icarus 1993;105:175-83. http://doi.org/10.1006/icar.1993.1117.

[7] Hellmann R, Bich E, Vesovic V. Cross second virial coefficients and dilute gas transport properties of the (CH_4+CO_2), (CH_4+H_2S), and (H_2S+CO_2) systems from accurate intermolecular potential energy surfaces. J Chem Phys 2016;102:429-41. https://doi.org/10.1016/j.jct.2016.07.034.

[8] Li X, Champagne MH, Hunt KLC. Long-range, collision-induced dipoles of T_d–D∞h molecule pairs: Theory and numerical results for CH_4 or CF_4 interacting with H_2, N_2, CO_2, or CS_2. J Chem Phys 1998;109:8416-25. https://doi.org/10.1063/1.477504

[9] Allen MP, Tildesley DJ . *Computer simulations of liquids*. Oxford University Press, Oxford (1987).
[10] Schofield P. Space-Time Correlation Function Formalism for Slow Neutron Scattering. Phys Rev Lett 1960;4:239-40. https://link.aps.org/doi/10.1103/PhysRevLett.4.239
[11] Hartmann J-M, Boulet C, Jacquemart D. Molecular dynamics simulations for CO_2 spectra. II. The far infrared collision-induced absorption band. J Chem Phys 2011;134:094316. https://doi.org/10.1063/1.3557681
[12] Bussery-Honvault B, Hartmann J-M. *Ab initio* calculations for the far infrared collision induced absorption by N_2 gas. J Chem Phys 2014 ;140 :054309. https://doi.org/10.1063/1.4863636
[13] Hartmann J-M, Boulet C, Toon GC. Collision-induced absorption by N_2 near 2.16 μm: Calculations, model, and consequences for atmospheric remote sensing, J Geophys Res Atmos 2017;122:2419-28. doi:10.1002/2016JD025677.
[14] Finenko A, Bezard B, Gordon I, Chistikov D, Lokshtanov S, Petrov S, Vigasin A. Trajectory-based simulation of far-infrared CIA profiles of CH_4-N_2 for modeling Titan's atmosphere. Astrophy J Suppl Series 2022;258:33. https://doi.org/10.3847/1538-4365/ac36d3
[15] Egelstaff PA. Neutron scattering studies of liquid diffusion. Adv Phys 1962;11:203-32. https://doi.org/10.1080/00018736200101282
[16] Mountain RD, Birnbaum G. Molecular dynamics study of intercollisional interference in collision-induced absorption in compressed fluids. J Chem Soc, Faraday Trans 2 1987;83:1791-99.
[17] Borysow A, Moraldi M. On the symetrization of rotational spectra for freely rotating linear molecules. Mol Phys 1994;82:1277-9. https://doi.org/10.1080/00268979400100904
[18] Birnbaum G, Borysow A, Buechele A. Collision-induced absorption in mixtures of symmetrical linear and tetrahedral molecules: Methane–nitrogen. J Chem Phys 1993;99:3234-43. https://doi.org/10.1063/1.465132
[19] Ahlrichs R, Penco P, Scoles G. Intermolecular forces in simple systems. Chem Phys 1977;19:119-30. https://doi.org/10.1016/0301-0104(77)85124-0
[20] Birnbaum G, Mountain RD. Molecular dynamics study of collision induced absorption in rare gas liquid mixtures. J Chem Phys 1984;81:2347-51. https://doi.org/10.1063/1.447933
[21] Bastien LA, Phillip NP, Brown NJ. Intermolecular potential parameters and combining rules determined from viscosity data. Int J Chem Kinet 2010;42:713-23. https://doi.org/10.1002/kin.20521
[22] Hellmann R, Bich E, Vogel E, Vesovic V. Intermolecular potential energy surface and thermophysical properties of the CH_4–N_2 system. J Chem Phys 2014;141:224301. https://doi.org/10.1063/1.4902807
[23] Karman T, Miliordos E, Hunt KLC, Groenenboom GC, van der Avoird A. Quantum mechanical calculation of the collision-induced absorption spectra of N_2-N_2 with anisotropic interactions. J Chem Phys 2015;142:084306. https://doi.org/10.1063/1.4907917
[24] Gustafsson M, Frommhold L. Infrared absorption spectra by H2–He collisional complexes: The effect of the anisotropy of the interaction potential. J Chem Phys 2000;113:3641-50. https://doi.org/10.1063/1.1287822
[25] Godin PJ, Ramirez RM, Campbell CL, Wizenberg T, Nguyen TG, Strong K, Moores JE. Collision-induced absorption of CH_4-CO_2 and H_2-CO_2 complexes and their effect on the ancient Martian atmosphere. J Geophys Res Planets 2020 ;125 :e2019JE006357. https://doi.org/10.1029/2019JE006357
[26] Finenko AA. Chistikov DN, Kalugina YN,. Conway EK, Gordon IE. Fitting potential energy and induced dipole surfaces of the van der Waals complex CH_4–N_2 using non-product quadrature grids. Phys Chem Chem Phys 2021; 23:18475-94. http://dx.doi.org/10.1039/D1CP02161C